VALIDATION OF FLUENT SOFTWARE FOR PREDICTION OF FLOW DISTRIBUTION AND PRESSURE GRADIENTS IN A MULTI-BRANCH FLOW HEADER

Ala Muhana and David Novog
Department of Engineering Physics, McMaster University
Hamilton, Ontario, Canada, 2008

Abstract

Flow headers are commonly used in nuclear reactors, boilers and heat exchangers to distribute fluid to small branches along the body of the header or to combine flow from the branches along the header. Historically, nuclear safety analysis has been performed using one-dimensional averaged system codes, and as such the distribution headers are cross-sectionally averaged. In this paper, flow distribution and pressure gradients along a multi-branch header have been predicted using the three dimensional computational fluid dynamics software FLUENT and were compared to results obtained from experimental data obtained from literature for single phase conditions. Water inlet flow rate through the header was varied and flow rates in the header branches were measured. The inlet flow rate was found to affect the flow distribution especially at low flow rates and the header pressure gradient especially at high flow rates. The aim of this work is to validate FLUENT software in predicting flow distribution and pressure gradients in single phase flow in such a multi-branch geometry. The effects of flow model, grid density, convergence criteria, flow inlet velocity and header size on the computational results were studied. For the impact of grid density, coarse, fine and very fine meshes were used and the mesh size beyond which no change in solution occurred was adopted. The impact of convergence criteria was studied by tightening the pressure and momentum relaxation factors as well as by decreasing the tolerance. The laminar model provided the best data fit in comparison with the standard and the RNG k-ε models. Vortex formation and flow separation were also studied and compared to the experimentally observed flow behaviour. Agreed with the experiment, largest vortices occur around the first branch pipe of the header.

Keywords: flow distribution, pressure gradients, flow header, FLUENT software, Computational Fluid Dynamics CFD.

1. Introduction

Equipments composed of headers and branch pipes for distributing a fluid stream or combining small streams are widely used in industry for fluids heating or cooling. In the Canada Deuterium Uranium CANDU Reactor, a main circulation pump takes cooled water from a steam generator and pumps it to an inlet header. The inlet header distributes the coolant through feeder pipes to individual fuel channels. Pressure tubes running through the reactor contain the fuel and coolant water passes through the pressure tubes and over the fuel. Hot water leaves the channels and collects in an outlet header and from there it goes to a second steam generator. The cooled water continues from the steam generator outlet to a second pump from where it is pumped through another set of headers, feeders and fuel channels back to the first steam generator. Another application in which the study of flow and pressure distributions along headers is important is in boilers and heat exchangers where horizontal headers are used to distribute the flow of a fluid to branches. The branches contribute to raise the heat transfer and thermal efficiency of the heat exchange system [1].

In the thermal hydraulic analysis of the nuclear reactor primary heat transport system PHTS it is generally assumed that the pressure distribution along the inlet and the outlet headers is uniform. As a result, the calculated flow in the channels between the two headers is also uniform since the channels are exposed to the same pressure difference. However, recent NUCIRC code predictions have shown that the pressure along the inlet header could vary by a value of up to 83 kPa [2]. Formulas were derived in the past to calculate the flow rate in each branch in multi-branch headers taking into consideration the diffuser effect on divided flow and the nozzle effect on confluent flow. Divided and confluent flow factors were experimentally determined and it was possible to calculate the flow in each branch pipe in cases where the inlet or the outlet of the header was placed between closed header ends [3]. The one-dimensional NUCIRC code was then modified to model the newer design of the CANDU reactor (large scale). A simulation code for the non-manifold and the manifold in the large scale reactor was developed [4]. Better loss coefficient predictions were provided and thus better determination of the header-to-header pressure drop in each fuel channel was obtained. The code was also able to capture any symmetries in the reactor PHTS using the modified manifold model. However, the predictions were still inaccurate as a result of the averaging.

Analytical models to obtain better predictions were also developed. The flow rates in the channels and the pressure difference across the header could be predicted by the solution of two pressure-flow ordinary differential equations. The header was divided into several basic combining flow manifolds, and the pressure-flow equations set was solved using an iterative procedure to satisfy the flow and pressure conditions at each junction point between the manifolds. Chandraker *et al.* [5] validated their model for a Pressurized Heavy Water Reactor PHWR against experimental data of flow and pressure with (i) both header turrets were open and (ii) one of the turrets was closed as well as pressure variations for different models of pump operation. Good agreement between the analytical and the experimental results was noticed.

Several studies have been carried out to investigate the accuracy of computational fluid dynamic CFD simulations in predicting flow distributions and pressure gradients in such multi-branch geometries. The effects of grid density and number of iterations on the computational results were studied. By comparing the results of one- and three-dimensional calculations of pressure and flow distributions inside a CANDU-6 reactor inlet header, it was found that the three-dimensional effects were able to capture some variations between feeders pressures in a given header cross-section, especially near the pump discharge pipe (the junction of the inlet turret and the header) [2]. Thus, the one-dimensional calculations for the CANDU-6 reactor headers should be further refined. The validity of using CFD results in a header-to-branch flow as a series of experimental results to develop a correlation that can be implemented to one dimensional accident analysis codes instead of doing experiments was also examined [6]. The physical modeling of transient experiments was implemented into the three-dimensional CFX10 software and it was found that the CFD results could be successfully used to develop the correlation. In a recent study, FLUENT was used to simulate two-phase flow behavior under low flow conditions in a cylindrical header manifold [7]. By comparing vapor phase distribution obtained by FLUENT with experimental data, no match was noticed when FLUENT vapor-water mixture model was used. It was more convenient to use the discrete-phase model to simulate the vapor entrainment since it tracks every vapor bubble in its pathway. The discrete-phase model was also used to simulate feeder vapor entrainment and two-phase injection into the header turret. It was reported that the vapor-phase behavior found could be useful in accident analyses.

In this study, a computational fluid dynamic CFD analysis is conducted for a multi-branch header in order to predict flow and pressure distributions and vortex formation along the header. This work represents the preliminary investigation of FLUENT for simulation of CANDU header gradients. The computational results were compared to experimental data obtained from S. Horiki [1] for single phase flow conditions. The impact of flow model, grid density, convergence criteria, flow inlet velocity and header size on the solution was investigated.

2. Experimental Apparatus and Data

As mentioned above, the experimental data of flow distribution and pressure gradients along a flow header was obtained from the work of S. Horiki [1]. The experimental setup consists of a horizontal rectangular header with four vertical branch pipes. The dimensions of the header are 10×40×1000 mm and the branches are connected to the header at intervals of 130 mm. The distance between the entrance of the header and the first branch is 600 mm and this length is enough to ensure fully developed flow. The branches are 1000 mm in length and 10 mm in diameter.

A constant static head tank was used to supply the feed water. The flow rates of the outlet water were calculated by measuring the time needed to accumulate a known amount of water. The inlet flow Reynolds number was varied from 500 up to 5000, and the flow was assumed to be isothermal. The collected data consists of the flow rate in each branch pipe and the pressure difference between the inlets of the adjacent branches at each inlet velocity. A sketch of the setup is shown in Fig (1).

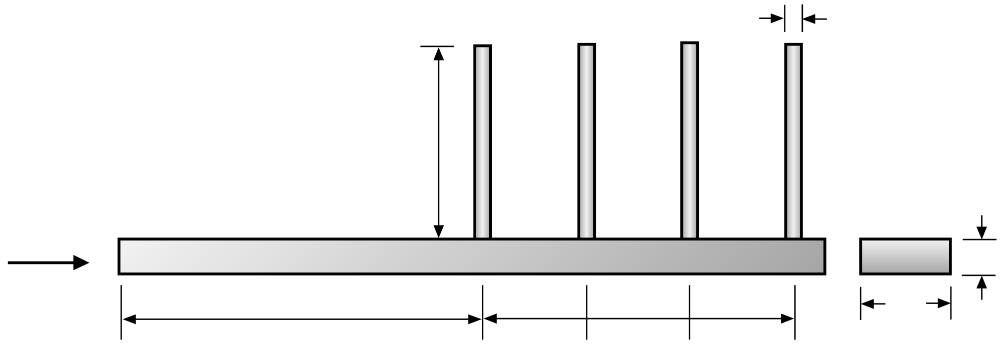

Fig (1): Sketch of the experimental setup (all dimensions are in mm).

3. Geometry, Mesh Generation

The geometry of the header was created using GAMBIT software. The code provides various shapes of geometrical objects that can be combined together to give the final desired geometry. The software can then be used to mesh the geometry for the CFD analysis and other scientific applications. The CFD analysis in this study was conducted using FLUENT. A sample of mesh created by GAMBIT is shown in Fig. (2). The mesh consists of $10\times10\times200$ header cells, 56,514 nodes, 143,633 faces. The total number of header and branch cells is 44,318.

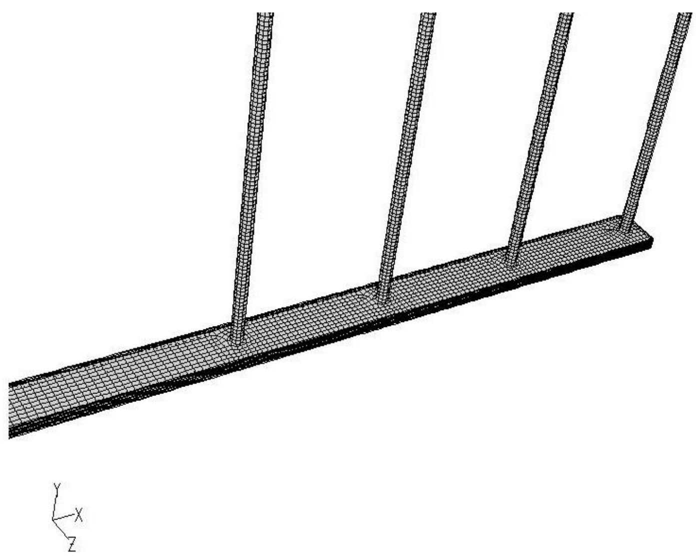

Fig. (2): Sample of mesh created by GAMBIT, 10×10×200 header cells, 56,514 nodes, 143,633 faces and a total of 44,318 cells.

4. Results and Discussion

4.1 Grid Density

To study the effect of grid density on the computational solution, different mesh sizes were used and the predictions of flow and pressure were compared together using the different mesh sizes. A coarse mesh of 6,576 nodes was initially used to obtain the solution. The mesh was then refined and the solution was compared with the one obtained using the previous mesh. This procedure was repeated until no change in the solution was noticed using two successive mesh sizes. The mesh size beyond which no change in solution occurred was considered adequate and used in the rest of this work. The selected mesh consists of 56,514 nodes. Fig. (3) shows the difference in average pressure at two planes just before the inlets of the first and the second branches obtained using the coarse mesh (line c) and the adopted mesh (line a) as well as a very fine mesh. The very fine mesh (line d) consists of 2,570,242 nodes. No difference in solution is noticed using the adopted and the very fine meshes.

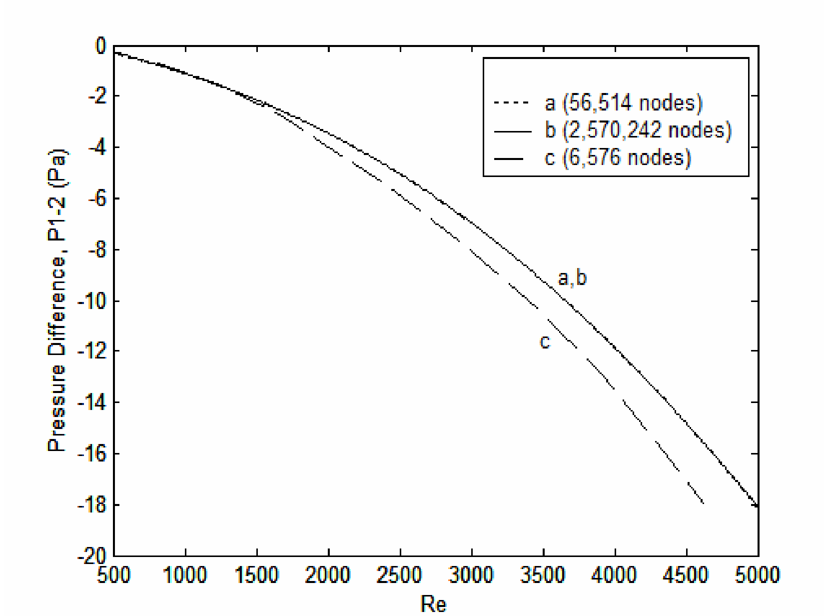

Fig. (3): Effect of mesh size on the pressure difference between two planes just before the inlets of the first two branches.

4.2 Flow Model

The experimental data available provides flow and pressure distributions along the header for a set of inlet water flow rates. The flow Reynolds number ranges from 500 to 5000. Both laminar and turbulence models were used for the analysis in this study to investigate the type of flow and to examine if a transition from laminar to turbulent flow occurs. Two turbulent models were tested; the standard and the RNG k-ε models. At the inlet, the turbulence intensity, k, and the turbulence dissipation, ε, were calculated as follows:

$$k = c_1 V^2, \quad \varepsilon = \frac{k^2}{c_2 D}$$

where V is the flow inlet velocity, D is the hydraulic diameter, and c1 and c2 are constants with the default values given by FLUENT (for each turbulence model).

Results of the solution are shown in Figures (4)-(6). In Fig (4), velocity contours are plotted at five different planes taken around the first branch Re=1217. The flow is laminar at plane A and it is more developed laminar flow at plane B. At plane C, just after the branch, the flow is disturbed as a result of water flow in the branch. The flow returns laminar downwards the branch as shown in plane D. To calculate the flow rates in FLUENT, a cross sectional plane was taken at the exit of each branch and the average flow rates across these planes were calculated. The same was done for pressure values prediction at planes just before the inlet of each branch. In Fig. (5), the ratio of the outlet flow rate in each branch to the total outlet flow rate was plotted versus the inlet flow Re number. The model predicts almost a uniform distribution in the branches. For low Re numbers, the model under-predicts the flow in the first branch and over-predicts the flow in the fourth branch. Attempts were made to improve the model prediction at low Re and the results of these attempts are discussed in section 4.3 below. However, the model prediction here is very close to the model prediction in the work of Horiki et al. [1]. The laminar model was found to provide the best data fit in Re range of this study. The standard and the RNG k-ε models provided the best data fit for the last three data points but the laminar model fits are still better. Thus, the laminar model was adopted in the rest of the work.

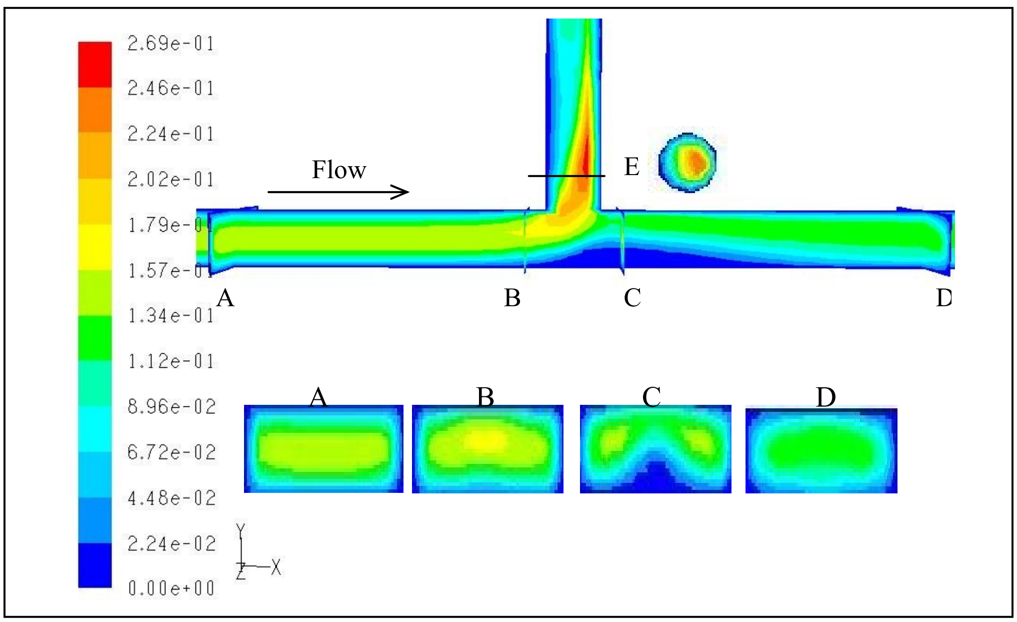

Fig. (4): Velocity contours at planes A, B, C, D and E around the first branch (Re=1217).

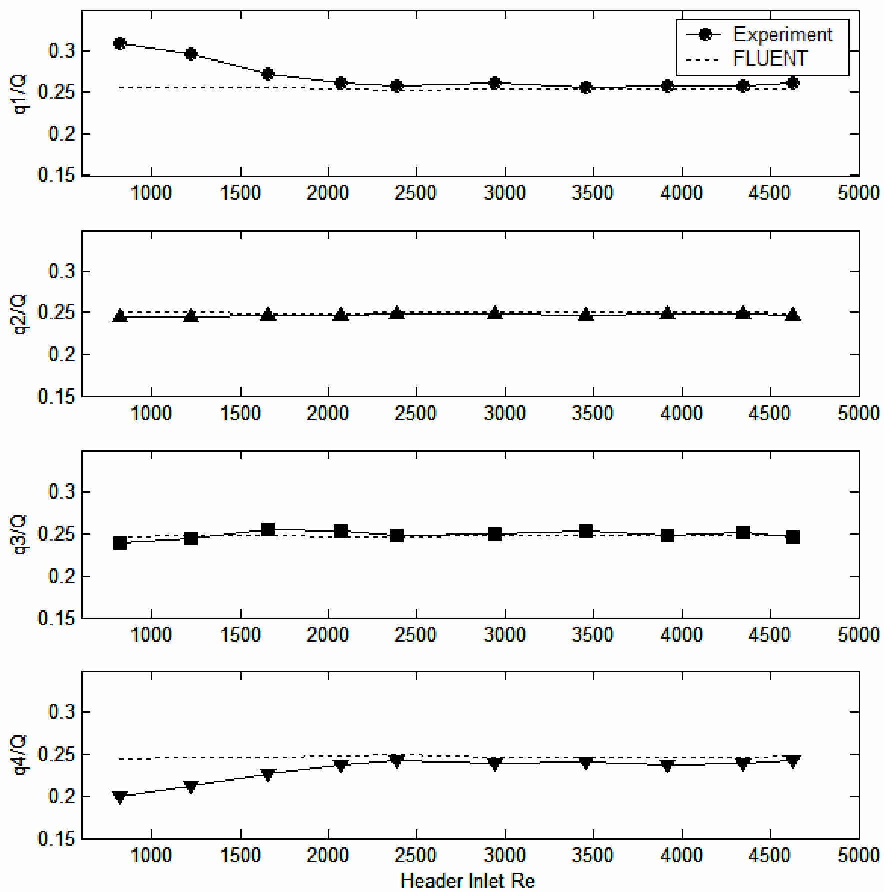

Fig. (5): Experimental data and FLUENT predictions of flow distribution in the branches as a function of inlet Re number.

The flow distribution in the branches for three selected Re numbers (Re=2943, 3457 and 4343) are plotted versus the branch number in Fig. (6). As Re number increases, the flow in the first two branches decreases and the flow in the last two branches increases. This behavior may be due to the higher pressure pushing the fluid towards the end of the header at high Re values. Similar behavior was also noticed for other Re numbers.

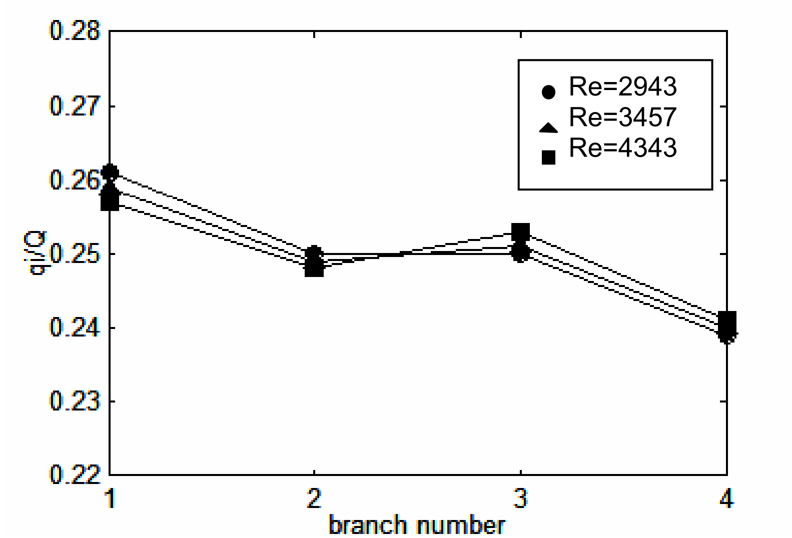

Fig. (6): Flow distribution in the branches at different Re numbers.

FLUENT 6.3 running time for each of the above computational cases (using the adopted mesh) was not more than 40 minutes using a 1.86 GHz processor. The tolerance was set to 10^{-4} and the pressure and momentum relaxation factors were set to their FLUENT default values. Incompressible, isothermal flow was assumed and pressure-based solver with implicit formulation was selected. In section 4.3 below, a sensitivity analysis to the convergence criteria was conducted where the relaxation factors were reduced. The maximum time for those simulations was around 12 hours using the very fine mesh.

4.3 Sensitivity Analysis

Convergence Criteria: Flow distribution and pressure gradients sensitivity analysis has been carried out using different convergence criteria. The relaxation factors of pressure and momentum were successively reduced from their FLUENT default values (0.3 and 0.7, respectively) and the effect of this tightening on the solution was observed. The tolerance was set to 10^{-3}, the FLUENT default value while reducing the relaxation factors. The maximum change in the solution was found to be only 0.47% in q_1/Q when the relaxation factors were tightened by 50% from the default values. The relaxation factors were more tightened and the maximum change in solution was only 0.04%. Then the tolerance was reduced to 10^{-4} and again very small change in solution was noticed. It is concluded that tightening the pressure and momentum relaxation factors by 75% of their default values with a tolerance of 10^{-4} is precise enough for the present study since no significant change in solution occurs by further tightening. If significant changes had been found, more tightening would be necessary.

Mesh Size: As was discussed in section 4.1, the mesh size choice was made by performing several simulations using different mesh sizes and the mesh size beyond which no change in solution occurred was adopted. However, attempting to predict the flow distribution as it was experimentally found at low Re numbers, the mesh size was decreased to get a very fine mesh around the branch inlets. It is expected that the more refined the grid near the branch inlets the more accurate the prediction. In the new mesh, the number of nodes around each branch inlet was more than 500,000 nodes with a total number of 2,570,242 nodes in the header. However, no improvement was noticed in the solution and again the almost uniform flow distribution was obtained (see fig (5)). The average run time for these simulations was around 10 hours.

The sensitivity analysis thus showed that no improvement in solution could be obtained by changing the convergence criteria and by using a very fine mesh near the inlets of the branches. However, the model predictions here are very close to the model predictions obtained by Horiki *et al.* [1] in their study. In another study, Horiki *et al.* [8] mentioned that the non-uniform behaviour in the experimental data at low Re numbers are considered to be due to flow instability in the distribution system. They explained that as the pressure in the header is considerably smaller at the low Re numbers, the flow distribution can be strongly affected by the local effluent condition at the outlet of the branches.

4.4 Pressure Gradients

Fig. (7) below shows contours of the dynamic pressure (Pa) in five different planes around the first branch at Re=1217.

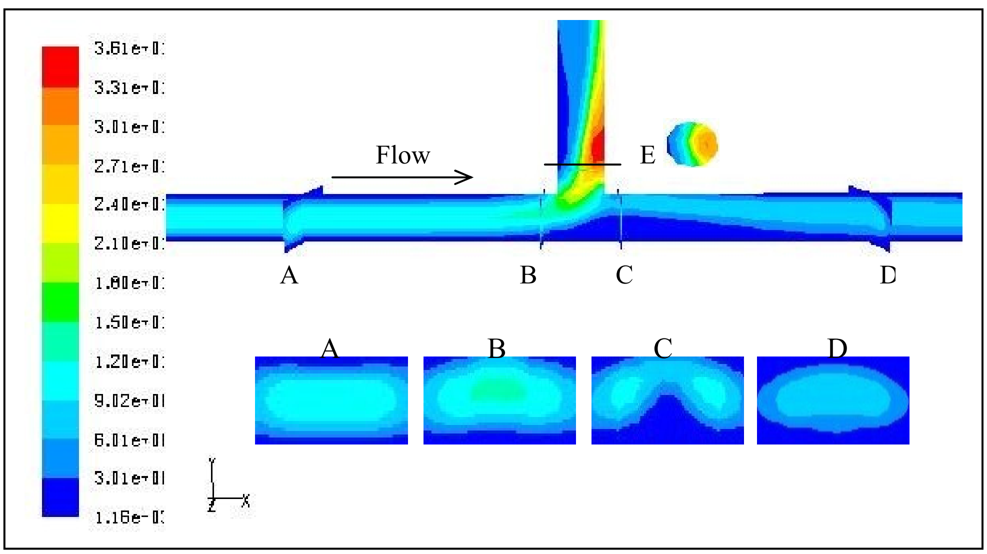

Fig. (7): Contours of dynamic pressure at planes A, B, C, D and E around the first branch (Re=1217).

Horiki et al. [1] used the experimentally obtained data of flow distribution in the branch pipes to calculate the pressure gradients in the header. Using the measured flow rates in the branches, flow velocities u_i and u_{i+1} at points i and $i+1$ before and after branch i were calculated. The pressure difference $p_{i+1}-p_i$ between these two points was then calculated as follows:

$$p_{i+1} - p_i = \eta \frac{\rho}{2}(u_i^{\,2} - u_{i+1}^{\,2}) - 4\lambda \frac{L}{D} \frac{\rho u_{i+1}^{\,2}}{2}$$

where η is a pressure recovery coefficient, ρ is density, λ is friction loss coefficient, L is interval length between branch pipes and D is the hydraulic diameter of the header. In their calculations, η was set to 1. The friction loss coefficient was calculated using Re number. The pressure differences were re-calculated using flow distribution experimental data in the above equation. The re-calculation was done because the scale of the pressure plot in their paper is large and the plot is too dense to obtain accurate readings. The obtained results were compared to FLUENT predictions as shown in Fig. (8). Good agreement between the model predictions and the experiment was noticed. The pressure differences are low for low Re numbers and high for higher Re numbers. This may be due to the increased amount of flow separation and vortex formation near the entrances of the branches as Re number increases. This phenomenon is discussed in section 4.5 below.

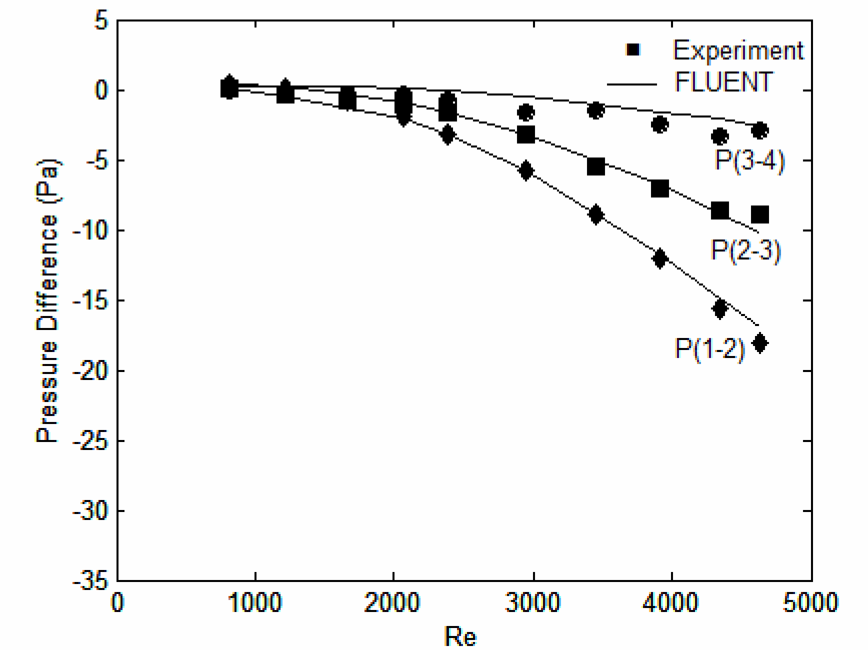

Fig. (8): Effect of inlet flow rate on the pressure gradients along the header.

4.5 Flow Separation and Vortex Formation

The header and the branch pipes used in the experimental study were made of transparent acrylic resin for the observation of the flow pattern. The flow pattern was visualized by injecting aluminum particles of about 2 μm in size at the header inlet. At Re=5000, it was found that flow separations occurred just after the branch pipes due to the water absorbed into the branch pipes. Also, vortices were observed inside the branch pipes. The largest vortex was observed at the inlet of the first branch pipe. Using FLUENT, contours of vortex magnitudes in the header were plotted for a Re number of 5000 as shown in Fig. (9). As was found in Horiki experiment, the largest vortex occurs at the inlet of the first branch pipe. The vortex magnitude decreases for the other branches as the flow velocity decreases through the header. A cross section plane of the first branch pipe showing the vortex contours inside the branch is also shown in Fig. (9).

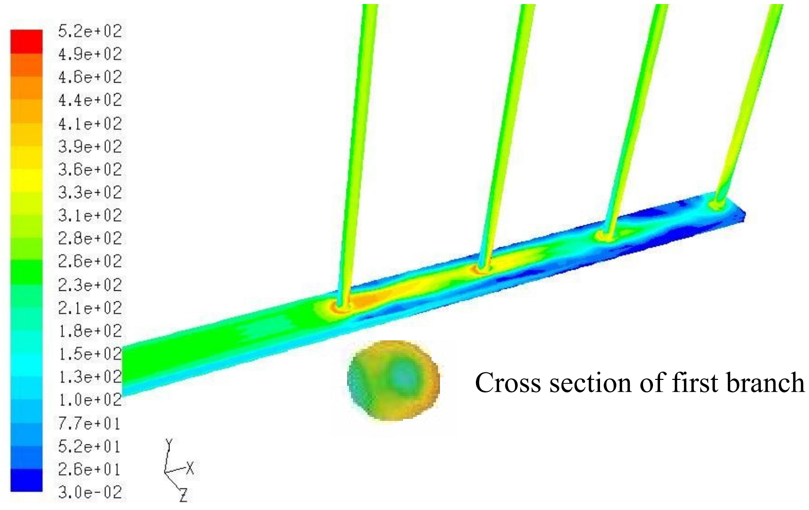

Fig. (9): Contours of vortex magnitude (Re=5000).

4.6 Header size

In their study, Horiki *et al.* [1] measured the flow distribution in a 10 mm × 40 mm header and in their study [8] they calculated the distribution in different sized headers. Fig. (10) and Fig. (11) show a comparison between their results (experimental and calculated) and FLUENT predictions obtained in this study. Fig (10) presents the effect of branch pipe length on the flow distribution in the 40 mm× 40 mm header at Re=4000, where h is the branch length. Fig. (11) represents the effect of the header size on the flow distribution. The flow distribution in the 10 mm × 40 mm header was experimentally measured but they theoretically calculated the distribution in the 40 mm× 40 mm header. FLUENT provided good prediction of the experimental data of the 10 mm× 40 mm header. For the 40 mm× 40 mm header, FLUENT over predicted Horiki calculations in the first two branches and under predicted it in the last two branches. This may be due to the three dimensional effects of FLUENT and the assumptions they made in their calculations (neglecting the higher order flows in the momentum equation) to estimate the values of the pressure recovery and the inlet distribution loss coefficients.

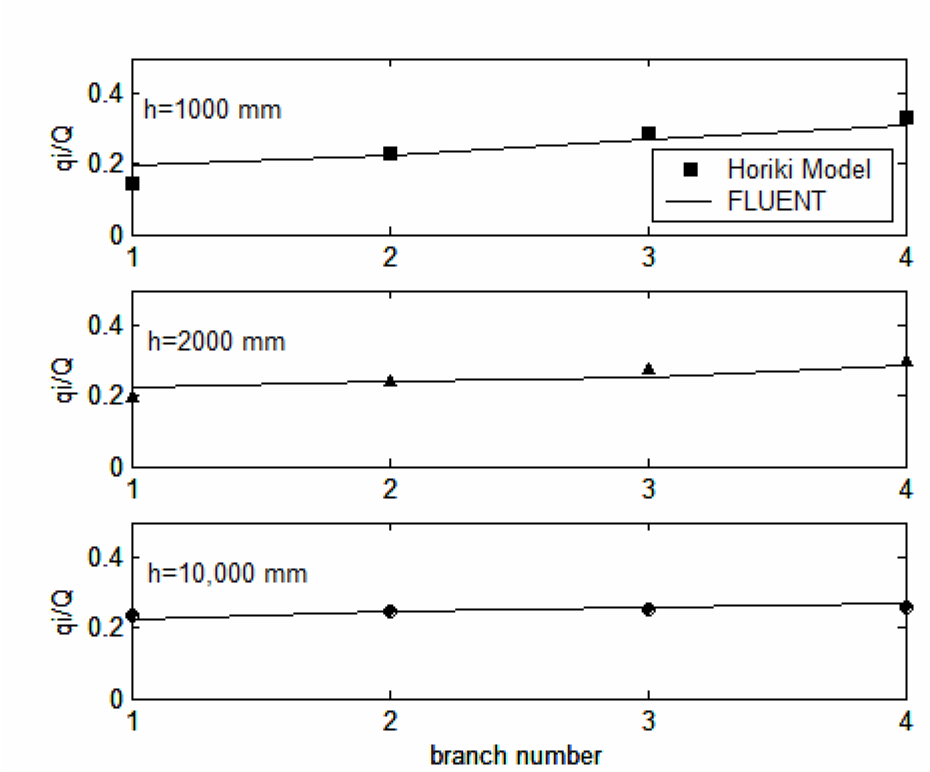

Fig. (10): Effect of branch length on flow distribution (Re=4000).

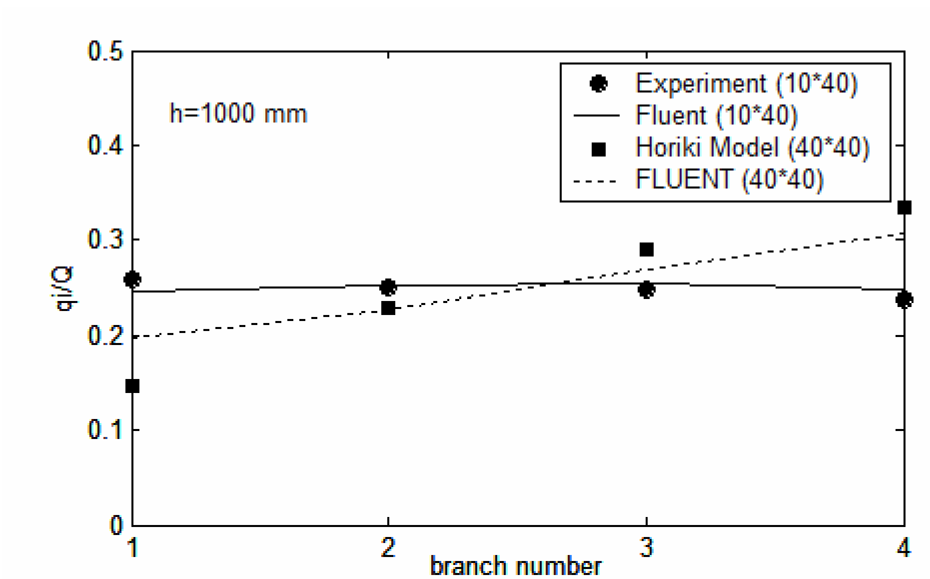

Fig. (11): Effect of header size on flow distribution (Re=4000).

5. Conclusions

Computational fluid dynamics CFD analysis of flow and pressure distributions in a multi-branch flow header using FLUENT software provided good prediction of experimental data obtained under a range of inlet water flow rates. The agreement between FLUENT predictions and experimental data indicates that FLUENT is an efficient tool to predict flow and pressure distributions in geometries of multi-branch headers.

6. References:

[1] S. Horiki, T. Nakamura and M. Osakabe, "**Thin Flow Header to Distribute Feed Water for Compact Heat Exchanger**", Experimental Thermal and Fluid Science 28, pp 201–207, 2004.

[2] R. Moffett, M. Soulard, G. Hotte, R. Gibb and A. Banas, "**Pressure Distribution Inside a CANDU-6 Reactor Inlet Header**", 4th Annual Conference of the CFD Society of Canada, Ottawa, Ontario, Canada, June 2-6, 1996.

[3] T. Kubo and T. Ueda, "**On the Characteristics of Divided Flow and Confluent Flow in Headers**", The Japan Society of Mechanical Engineers, 12, No. 52, pp. 802-809, 1969.

[4] A. Kwan, "**Modeling of a Header for the CANDU Primary Heat Transport System**", Master Degree Thesis in Engineering Physics, McMaster University, Hamilton, Ontario, Canada, 1997.

[5] D. Chandraker, N. Maheshwari, D. Saha and V. Venkat Raj, "**Experimental and Analytical Investigation on Core Flow Distribution and Pressure Distribution in the Outlet Header of a PHWR**", Experimental Thermal and Fluid Science, 27 (11–24), 2002.

[6] Yong Jin Cho, In Goo Kim and Gyoo Dong Jeun, "**Application of CFD Technique to CANDU Header-to-Feeder Free Surface Flow",** NTHAS5: Fifth Korea-Japan Symposium on Nuclear Thermal Hydraulics and Safety, Jeju, Korea, November 26- 29, 2006.

[7] P. Gulshani, "**Investigation of Natural Circulation Two-Phase Flow Behaviour in Header Manifold using CFD Code**", 27th Annual Conference of Canadian Nuclear Society, Toronto, Ontario, Canada, June 11 - 14, 2006.

[8] M. Osakabe, T. Hamada and S. Horiki, "**Water Flow Distribution in Horizontal Header Contaminated with Bubbles**", International Journal of Multiphase Flow 25, pp. 827-840, 1999.

APPENDIX A: ABBREVIATIONS

Abbreviation	Meaning
RNG	Re-Normalization Grouping
CFD	Computational Fluid Dynamics
PHTS	Primary Heat Transport System
CANDU	Canada Deuterium / Uranium

APPENDIX B: COEFFICIENTS AND PARAMETERS

Parameter/Coefficient	Description
k	Turbulence intensity
ε	Turbulence dissipation
c_1	Turbulence intensity constant
c_2	Turbulence dissipation constant
V	Inlet flow velocity (m/s)
D	Hydraulic diameter (m)
Q	Inlet flow rate (m^3/s)
q_i	Outlet flow rate in branch i (m^3/s)